Original Article | Thoracic Imaging

http://dx.doi.org/10.3348/kjr.2016.17.5.684
pISSN 1229-6929 · eISSN 2005-8330
Korean J Radiol 2016;17(5):684-694

Korean Journal of Radiology
KJR

Diagnosing Lung Nodules on Oncologic MR/PET Imaging: Comparison of Fast T1-Weighted Sequences and Influence of Image Acquisition in Inspiration and Expiration Breath-Hold

Nina F. Schwenzer, MD[1], Ferdinand Seith, MD[1], Sergios Gatidis, MD[1], Cornelia Brendle, MD[1, 2], Holger Schmidt, PhD[1], Christina A. Pfannenberg, MD[1], Christian laFougère, MD[3], Konstantin Nikolaou, MD[1], Christina Schraml, MD[1]

Departments of [1]Diagnostic and Interventional Radiology, [2]Diagnostic and Interventional Neuroradiology, and [3]Nuclear Medicine, University Hospital of Tuebingen, Tuebingen 72076, Germany

Objective: First, to investigate the diagnostic performance of fast T1-weighted sequences for lung nodule evaluation in oncologic magnetic resonance (MR)/positron emission tomography (PET). Second, to evaluate the influence of image acquisition in inspiration and expiration breath-hold on diagnostic performance.

Materials and Methods: The study was approved by the local Institutional Review Board. PET/CT and MR/PET of 44 cancer patients were evaluated by 2 readers. PET/CT included lung computed tomography (CT) scans in inspiration and expiration (CTin, CTex). MR/PET included Dixon sequence for attenuation correction and fast T1-weighted volumetric interpolated breath-hold examination (VIBE) sequences (volume interpolated breath-hold examination acquired in inspiration [VIBEin], volume interpolated breath-hold examination acquired in expiration [VIBEex]). Diagnostic performance was analyzed for lesion-, lobe-, and size-dependence. Diagnostic confidence was evaluated (4-point Likert-scale; 1 = high). Jackknife alternative free-response receiver-operating characteristic (JAFROC) analysis was performed.

Results: Seventy-six pulmonary lesions were evaluated. Lesion-based detection rates were: CTex, 77.6%; VIBEin, 53.3%; VIBEex, 51.3%; and Dixon, 22.4%. Lobe-based detection rates were: CTex, 89.6%; VIBEin, 58.3%; VIBEex, 60.4%; and Dixon, 31.3%. In contrast to CT, inspiration versus expiration did not alter diagnostic performance in VIBE sequences. Diagnostic confidence was best for VIBEin and CTex and decreased in VIBEex and Dixon (1.2 ± 0.6; 1.2 ± 0.7; 1.5 ± 0.9; 1.7 ± 1.1, respectively). The JAFROC figure-of-merit of Dixon was significantly lower. All patients with malignant lesions were identified by CTex, VIBEin, and VIBEex, while 3 patients were false-negative in Dixon.

Conclusion: Fast T1-weighted VIBE sequences allow for identification of patients with malignant pulmonary lesions. The Dixon sequence is not recommended for lung nodule evaluation in oncologic MR/PET patients. In contrast to CT, inspiration versus expiratory breath-hold in VIBE sequences was less crucial for lung nodule evaluation but was important for diagnostic confidence.

Keywords: *PET/MR; PET/MRI; MR/PET; Lung; Pulmonary nodule; Inspiration; Expiration*

Received December 5, 2015; accepted after revision April 26, 2016.
Corresponding author: Christina Schraml, MD, Department of Diagnostic and Interventional Radiology, University Hospital of Tuebingen, Hoppe-Seyler-Str. 3, Tuebingen 72076, Germany.
• Tel: (49) 7071 29 82087 • Fax: (49) 7071 29 5845
• E-mail: christina.schraml@med.uni-tuebingen.de

INTRODUCTION

Recently, whole-body integrated magnetic resonance/positron emission tomography (MR/PET) systems have been introduced in the clinical routine (1). Major advantages of MR/PET over PET/CT are the improved soft-tissue contrast, motion correction, alignment quality, bone marrow evaluation and the reduced radiation exposure with potential improvement of care in cancer patients (2-7). In

Korean Journal of Radiology
KJR

oncologic whole-body imaging, the evaluation of pulmonary lesions plays an important role for staging and treatment decisions. This raises the question of MR/PET performance for the evaluation of lung nodules in cancer patients, in comparison to PET/CT.

State-of-the-art MRI lung protocols comprise fast T1-weighted three-dimensional (3D) gradient-echo sequences, fast spin-echo T2-weighted sequences and steady-state gradient-echo sequences (8, 9). In recent years, MR sequences with radial stack-of-stars trajectory indicated promising fields of applications also in MR/PET (10, 11). However, to date, the scan times of radial sequences are within the range of minutes. Thus, depending on the individual diagnostic task, a thoracic MR protocol may still last up to 20–30 minutes (8). Due to the limited MR acquisition time in oncologic whole-body MR/PET imaging, it is desirable to use a sequence type that offers high spatial resolution for lung lesion detection and large scan volume coverage in a short time. For these reasons, modified breath-hold 3D gradient-echo MRI sequences were established (12-14) with different acronyms depending on the vendor (T1-weighted volumetric interpolated breath-hold examination [VIBE], T1 high resolution isotropic volume excitation or liver acquisition with volume acceleration). In contrast to the above-described sequences, the 2-point Dixon sequence obtained for attenuation correction (AC) of the PET data in whole-body MR/PET has also been proposed for anatomical allocation of lung lesions (15).

For PET/CT, it was demonstrated that the best co-registration quality between PET and CT can be achieved under expiration, under mid-suspend breath-hold or under shallow breathing (16-19). Thus, an additional chest CT scan in inspiration (CTin) is frequently performed in oncologic PET/CT examinations because the detection rate for small pulmonary lesions can be significantly improved, as compared to a CT scan in expiration alone (17).

Therefore, the aim of the study was twofold: primarily, to investigate the diagnostic performance of fast T1-weighted sequences for pulmonary nodule evaluation in oncologic MR/PET patients. Second, to evaluate the influence of image acquisition in inspiration and expiration breath-hold on diagnostic performance.

MATERIALS AND METHODS

Patients

The study was approved by the local Institutional Review Board. All patients gave written informed consent. Retrospective analysis of datasets of 44 oncological fluorodeoxyglucose (FDG)-MR/PET patients who underwent a clinically indicated PET/CT with subsequent voluntary MR/PET was performed (16 female; mean age, 55 ± 15 years). Inclusion criteria were PET/CT and MR/PET examinations on the same day with coverage of the lung, oncological referral with fluorine 18 (^{18}F)-FDG as radiotracer, CT in inspiration in PET/CT, VIBE in inspiration and expiration in PET/MR. Details for patient flow were given in Figure 1. Clinical indication for PET/CT was staging or follow-up of the following diseases: lung cancer (n = 10), melanoma (n = 11), thyroid cancer (n = 9), lymphoma (n = 3), oesophageal cancer (n = 2), sarcoma (n = 2), cancer of unknown primary (n = 2), tongue carcinoma (n = 1), oropharyngeal cancer (n = 1), laryngeal cancer (n = 1), colorectal cancer (n = 1), breast cancer (n = 1).

MR/PET and PET/CT Protocol

All patients fasted overnight before administration of the glucose analogue ^{18}F-FDG. The radiotracer was injected in the PET/CT suite (mean dose ± standard deviation: 351 ± 22 MBq). Blood glucose was measured before injection to ensure blood glucose levels below 150 mg/dL. PET/CT

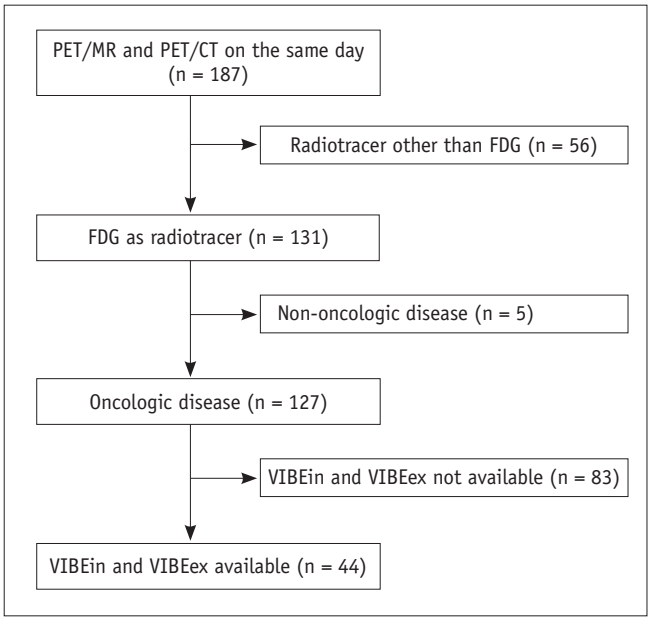

Fig. 1. Flow chart of patients. Diagram showing inclusion of patients evaluated in study (n = number of patients). FDG = fluorodeoxyglucose, PET/MR = positron emission tomography/magnetic resonance, VIBEex = volume interpolated breath-hold examination acquired in expiration, VIBEin = volume interpolated breath-hold examination acquired in inspiration

was conducted at a Biograph mCT (Siemens Healthcare, Knoxville, TN, USA) as whole-body examinations in expiration. CT-based attenuation maps were calculated using the vendor-provided algorithm. PET was acquired under free breathing and reconstructed with iterative 3D ordered-subset expectation maximization (OSEM) algorithm using 2 iterations and 21 subsets and a Gaussian filter of 2 mm. The PET was acquired with 2–4 minutes/bed depending on the body region.

MR/PET was performed immediately after PET/CT on a Biograph mMR (Siemens Healthcare, Erlangen, Germany). Mean uptake time in MR/PET was 124 ± 13 minutes. PET was acquired under free breathing and reconstructed with an iterative 3D OSEM algorithm using 3 iterations and 21 subsets and a Gaussian filter of 3 mm. Time per bed was 4–6 minutes.

A whole-body 3D T1-weighted spoiled gradient-echo sequence fast low angle shot in end-expiratory breath-hold with Dixon-based fat-water separation (Dixon, sequence parameters in Table 1) was acquired for the generation of a segmentation-based PET AC map.

Lung Imaging

In PET/CT, the thorax was covered in expiration as part of the whole-body examination (CT acquired in expiration [CTex]). In addition, a lung CT scan in inspiration (CTin) was performed, which is a standard operation procedure of the routine scan protocol in our institution. CT was reconstructed in axial orientation with slice thickness of 3 mm (CTin) and 5 mm (CTex) with an in-plane resolution of 0.8 x 0.8 mm^2. In MRI, axial VIBE sequences of the lung were acquired in inspiration and expiration (volume interpolated breath-hold examination acquired in inspiration [VIBEin], volume interpolated breath-hold examination acquired in expiration [VIBEex]). Lung images available from the whole-body Dixon sequence were also included in the evaluation. The 3D Dixon sequence was acquired in expiration for higher alignment quality with the PET data. Per default, the 3D Dixon sequence has to be acquired in coronal orientation. Detailed scan and reconstruction parameters for lung imaging were shown in Table 1.

Image Evaluation

Lung imaging was evaluated in consensus by 2 blinded radiologists experienced in thoracic (12 and 6 years) and hybrid imaging (6 and 4 years) including fellowships in nuclear medicine. Five separate reading sessions with different data sets were performed, each at least 8 weeks apart in a random order (CTex, VIBEin, VIBEex, and Dixon). Number, lobe and size of the lesions (longest diameter in lung window setting with window width, 1500 Hounsfield units [HU] and window level, -500 HU) were recorded for each patient. Confidence in the presence of a potentially malignant lesion was rated on a 4-point Likert scale (1, highly likely; 2, very likely; 3, probable; 4, uncertain) for each finding. Calcified nodules were not included in the analysis. PET was available in all reading sessions and PET images were visually analysed in combination with the morphological images to identify additional lesions only visible in PET.

The reference standard was defined in PET/CT with additional CT in inspiration by a third radiologist experienced in thoracic (11 years) and hybrid imaging (5 years) including fellowships in nuclear medicine. The third radiologist correlated the results (localization and confidence in presence of a lesion) of the 2 blinded readers in the different imaging modalities and performed a lesion-by-lesion comparison in all patients and recorded the detection of each lesion in VIBEin, VIBEex, CTex, and Dixon. Size (long axis diameter) of lesion was measured in

Table 1. Parameters of T1-Weighted MR Sequences Used for Lung Imaging

Parameter	3D Dixon	3D VIBE
Breath-hold position	Expiration	Inspiration/expiration
Orientation	Coronal*	Axial
TE (ms)	1.23/2.46	1.3
TR (ms)	3.6	3.4
TA (s)	19	17
Flip angle	10°	5°
Acquired image resolution (mm^3)	4.1 x 4.1 x 2.6*	1.2 x 0.9 x 6
Reconstructed voxel size (mm^3)	2.6 x 2.6 x 2.6*	0.9 x 0.9 x 3
Bandwidth (Hz/pixel)	965	543

*Orientation and matrix size is fixed by default by vendor because sequence is used to create μ-map for attenuation correction. TA = time of acquisition, TE = echo time, TR = repetition time, VIBE = volumetric interpolated breath-hold examination, 3D = three-dimensional

Korean Journal of Radiology
KJR

CTin in lung window settings. If the lesion was not found by the readers in each modality, it was considered as "false negative". A lesion was defined as false positive if the lesion was not rated as lesion in the reference standard, e.g., small atelectasis or vessel mistaken for pulmonary nodule.

Data Analysis

In a lesion-based analysis, detection rate (sensitivity) of each image data set (CTex, VIBEin, VIBEex, and Dixon) was calculated. Size-depending evaluation was performed according to the size ranges defined by the Fleischner society (≤ 4 mm; > 4 to ≤ 6 mm; > 6 to ≤ 8 mm; > 8 mm) (20). In a lobe-based analysis, sensitivity and specificity were calculated for each image data set. The lobe-based analysis was performed because it is important for tumor node metastasis (TNM) staging in lung cancer and for preoperative treatment planning in patients eligible for metastasectomy. In addition to the overall evaluation, a separate analysis of diagnostic parameters was performed considering only malignant pulmonary lesions as proven by follow-up or biopsy. When biopsy was not available, the follow-up data was used to classify a lesion as malignant. For this purpose, standard diagnostic criteria were applied such as increase in size.

Statistical Analysis

Patients with > 10 lesions per lung were excluded to prevent disproportionate contribution of one patient to the evaluation. The Kruskal-Wallis one-way analysis of variance with post-hoc test was performed to assess for differences in the diagnostic confidence in lesion delineation between the different reading sets. As post-hoc test, a non-parametric multiple comparison test available in SPSS (correction for multiple testing included) was conducted. McNemar test was used to compare the detection rate between VIBEin and VIBEex. These statistical analyses and graphs were performed using SPSS software package (version

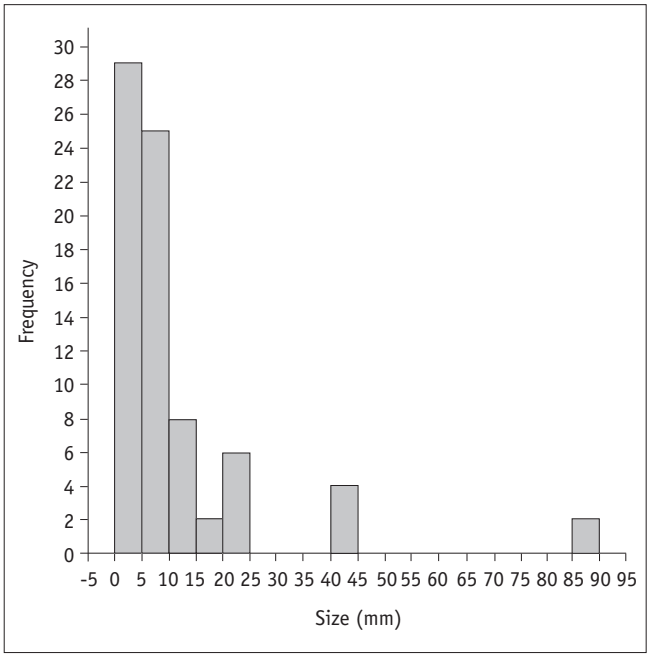

Fig. 2. Lesion size. Histogram showing frequency of lesion sizes for all 76 lesions found in 23 patients. Median lesion size was 6 mm; range was between 2 and 86 mm.

Table 2. Lesion-Based Analysis

	CTex	VIBEin	VIBEex	Dixon
Detection rate all lesions	77.6 (67.1–85.5)	55.3 (44.1–65.9)	51.3 (40.3–62.2)	22.4 (14.5–32.9)
Detection rate by nodule size*				
> 8 mm	91.7	87.5	87.5	62.5
> 6 to ≤ 8 mm	100	75	62.5	0
> 4 to ≤ 6 mm	93.3	66.7	66.7	13.3
≤ 4 mm	51.7	17.2	10.3	0

Values are given in percent together with 95% confidence interval in brackets. Specificity could not be calculated because there were no true negative pulmonary lesions. *Nodule size was measured in CT scan in inspiration (lung window setting). CTex = CT acquired in expiration, VIBEex = volume interpolated breath-hold examination acquired in expiration, VIBEin = volume interpolated breath-hold examination acquired in inspiration

Table 3. Lobe-Based Analysis

	CTex	VIBEin	VIBEex	Dixon
Sensitivity (CI)	89.6 (77.8–95.5)	58.3 (44.3–71.2)	60.4 (46.3–73.0)	31.3 (20.0–45.3)
Specificity (CI)	100 (97.6–100)	98.7 (95.5–99.7)	99.4 (96.5–99.9)	99.4 (96.5–99.9)

Values are given in percent with the 95% confidence intervals (CI) in brackets. On right side of table, *p* values for pairwise comparisons between different imaging techniques are given. CTex = CT acquired in expiration, VIBEex = volume interpolated breath-hold examination acquired in expiration, VIBEin = volume interpolated breath-hold examination acquired in inspiration

22.0.0, SPSS Inc., Chicago, IL, USA). Figures of merit (FOM) were calculated for each imaging set and compared using Jackknife FROC software (Jackknife alternative free-response receiver-operating characteristic, version 4.2.1; http://www.devchakraborty.com), which provides a specific analysis of observer free-response tasks (21, 22). $P < 0.05$ was considered statistically significant.

RESULTS

Three patients were excluded due to disseminated metastatic disease in both lungs (> 10 lesions per lung). In 23 of the evaluated 41 patients, 76 lung lesions were present as defined by the reference standard. On average, 3 ± 3 lesions (range: 1–18) per patient were found with a median lesion size of 6 mm (range: 2–86 mm). Size distribution of pulmonary lesions is given in Figure 2. Detection rates obtained in the lesion- and lobe-based analyses are given in Tables 2 and 3.

Lesion-Based Analysis

Compared to the reference standard, the lesion-based detection rate of all other modalities was inferior (CTex, 77.6%; VIBEin, 55.3%; VIBEex, 51.3%; and Dixon, 22.4%). In the size-dependent analysis, the detection rates of VIBE sequences ranged between 62.5 and 87.5% and dropped considerably for lesions ≤ 4 mm to 17.2% and 10.3% in VIBEin and VIBEex, respectively. In the Dixon sequence, lesions > 8 mm in size were missed in 38% of cases. In the lesion-based analysis, 5 false positive lesions were found in VIBEin, which could be ascribed to fibrotic and dystelectatic changes. In the Dixon sequence, 1 round atelectasis was falsely rated as lesion (Fig. 3). Adding the PET information to the different MR readings, an additional lung lesion was identified for the Dixon reading set, which was confirmed malignant in follow-up (Fig. 4); while using VIBEin or VIBEex sequences, no additional pulmonary lesion was found in PET.

Lobe-Based Analysis

In the lobe-based analysis, lesions were found in 48/204 lobes (in 1 patient, only 2 lobes were present on the right side after lobectomy). The lobe-based sensitivity of CTex and MRI sequences was generally higher compared to the lesion-based analysis and all T1-weighted MRI sequences still provided inferior detection rates than CT (CTex, 89.6%; VIBEin, 58.3%; VIBEex, 60.4%; and Dixon, 27.1%). In all reading sets (either CT or MRI), lung nodule evaluation showed high specificity (98.7–100%). Two lesions in the VIBEin sequence and 1 lesion in the VIBEex sequence were assigned to another lobe leading to 2 false positive cases in VIBEin and 1 false positive case in VIBEex in the lobe-based analysis. The erroneous lobe attribution occurred due to the limited identifiability of fissures in MRI (Fig. 5).

Diagnostic Confidence Analysis

The diagnostic confidence in lesion delineation was rated highest in VIBEin (1.2 ± 0.6) and CTex (1.2 ± 0.7) followed by VIBEex (1.5 ± 0.9) and Dixon (1.7 ± 1.1). In the post-hoc analysis, no statistical significant difference was found.

Figures of Merit

The diagnostic performance of the different imaging techniques as represented by FOMs is summarized in Table 4. CTex had a significantly higher FOM compared to VIBEin, VIBEex, and Dixon. The Dixon sequence had a significantly lower FOM compared to VIBEin, VIBEex, and CTex. FOM of VIBE in inspiration and expiration did not significantly differ.

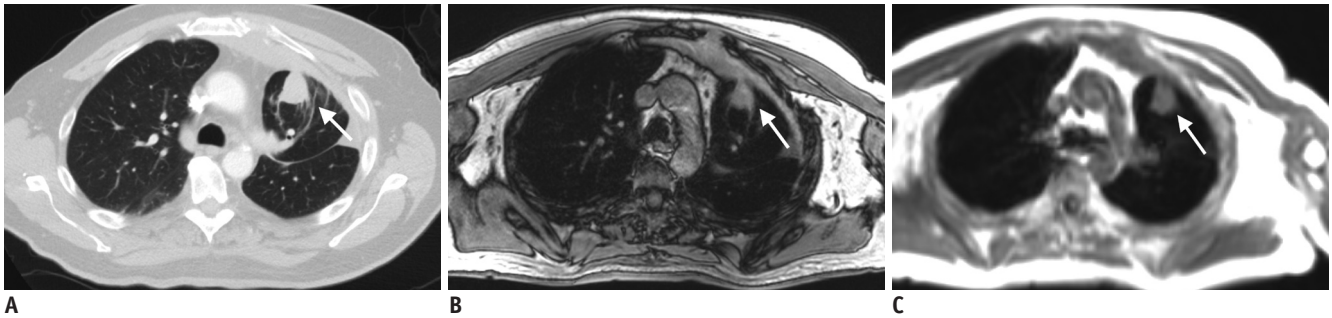

A B C

Fig. 3. 67-year-old male patient with lung cancer.
A. CT in inspiration. **B.** VIBE sequence in inspiration. **C.** Dixon sequence in expiration. In left upper lobe, round atelectasis is shown (arrow), which could easily be identified in CT as well as in VIBE sequence due characteristic comet sign. In Dixon sequence, atelectasis was rated as potentially malignant lesion with confidence rating of 2 (= very likely) leading to false positive lesion. VIBE = volume interpolated breath-hold examination

Korean Journal of Radiology
KJR

Separate Analysis of Malignant Pulmonary Lesions

In 17 of 23 patients with pulmonary lesions, follow-up or biopsy was available. In these 17 patients, 47 lesions were identified. Based on biopsy and follow-up, 33 of these 47 lesions were malignant (median lesion size: 8 mm, range: 2–86 mm). Taking into account only these proven malignant lesions, the lesion-based detection rate increased in all modalities irrespective of inspiration or expiration breath-hold imaging (CTex, 84.8%; VIBEin, 75.8%; VIBEex, 69.7%; and Dixon, 33.3%). Patient-based, it was possible to identify all patients with malignant lesions in CTex, VIBEin and VIBEex, although several single lesions were missed. In contrast, 3 patients were rated false-negative for malignant lesions based on the Dixon sequence alone (Fig. 6). Of these, one could be identified as having a lung nodule when adding the PET information (Fig. 4).

Influence of Image Acquisition in Inspiratory and Expiratory Breath-Hold

In contrast to CT, the percentage difference of lesion detection rates between inspiratory and expiratory breath-hold was small and not significant (3.9% between VIBEin and VIBEex versus 22.4% between CTin and CTex). Taking into account only the malignant lesions, the percentage difference of detection rates between VIBEin and VIBEex was slightly higher with 6.1%, without reaching significance (percentage difference between CTin and CTex: 15.2%).

DISCUSSION

In the present study, the diagnostic performance of standard fast T1-weighted images was investigated for lung nodule assessment in MR/PET imaging of cancer patients. Three different fast T1-weighted sequences commonly used in MR/PET were evaluated to assure large

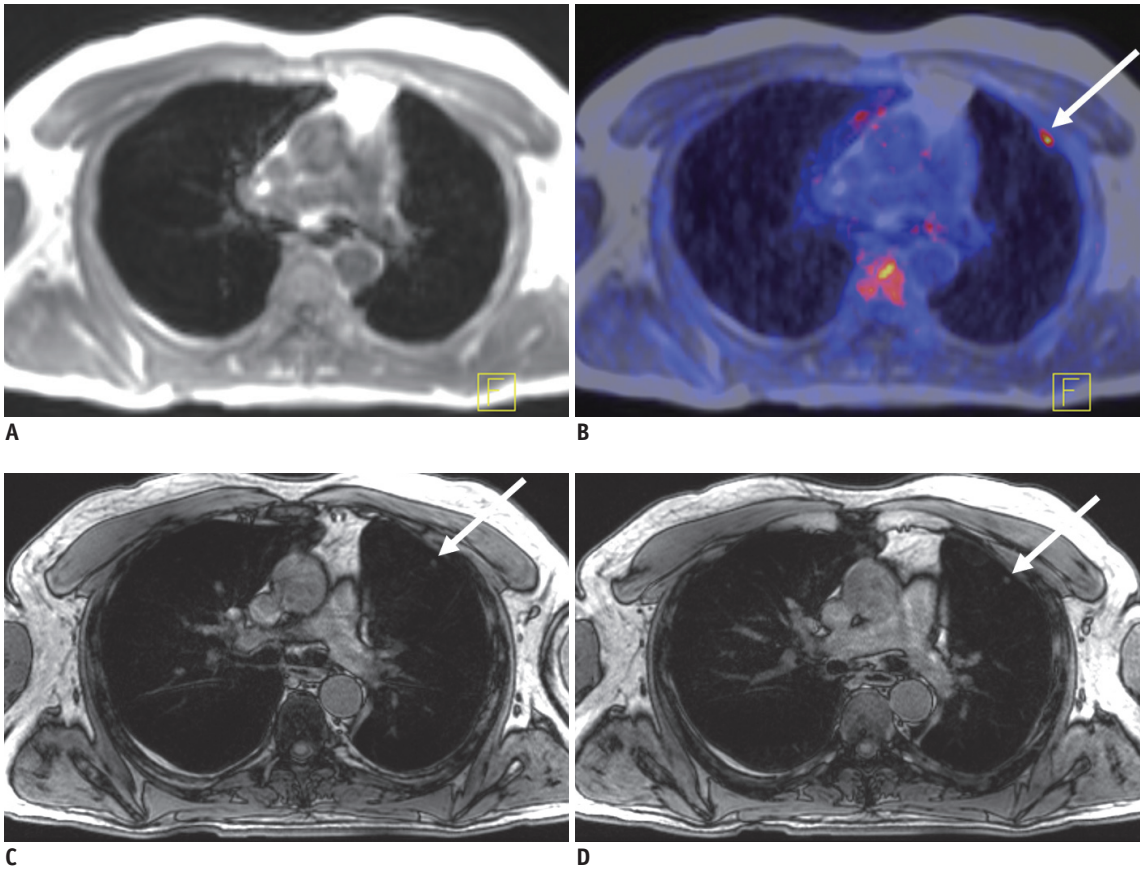

Fig. 4. 62-year-old male patient with thyroid cancer.
A. Dixon sequence in expiration. **B.** Fused PET/Dixon. **C.** VIBEin. **D.** VIBEex. In fused images, focal uptake was observed in periphery of left lung (arrow), which was rated as lesion based on PET information. In Dixon sequence, there was no correlate to finding while in VIBEin and VIBEex small subpleural nodule was visible, which was rated as potentially malignant with confidence level of 1 (= highly likely). In follow-up imaging, lesion grew in size and was rated as metastasis in standard of reference. PET = positron emission tomography, VIBEex = volume interpolated breath-hold examination acquired in expiration, VIBEin = volume interpolated breath-hold examination acquired in inspiration

clinical representativeness. The secondary focus was on the influence of the breath-hold in inspiration versus expiration, since scans in expiration are known to show higher alignment quality with PET (16, 23). In order to consider the diagnostic value for patient management, different evaluation perspectives were considered by performing lesion-, lobe- and patient-based analyses. Moreover, separate evaluation was performed for the different size categories of pulmonary lesions established by the Fleischner society (20).

To our knowledge, no systematic comparison of breath-hold positions used in dedicated VIBE sequences for lung imaging in MR/PET has been performed yet. PET/CT studies have shown that CT in expiration or shallow breathing is inferior in pulmonary lesion detection although it offers higher alignment quality to PET data (24, 25). This is in accordance with our study results. Interestingly, in contrast to CT, there was no substantial difference between breath-hold positions in the VIBE sequences. Thus, a dedicated lung VIBE sequence in expiration might be sufficient for the assessment of pulmonary lesions in oncologic MR/PET protocols.

In the lesion-based analysis, CT (either in inspiration or expiration) was superior compared to MRI. However, the detection rate in MRI markedly increased when only malignant lesions were taken into account (VIBEin: 76% vs. 55%). In the patient-based evaluation, no patient with pulmonary lesions was missed using the dedicated VIBE sequence irrespective of the breath-hold position. Recently, Raad et al. (11) showed that most pulmonary lesions (97%) missed on MR/PET were stable or vanished in follow-up imaging indicating their benign nature. This observation is also reflected by our data.

In our study, the overall detection rate of VIBEin was 55%, which is below detection rates reported in the literature: Chandarana et al. (26) found a detection rate of 62% using a radial VIBE sequence in an integrated MR/PET. Rauscher et al. (27) report a detection rate of 68% using a VIBE sequence in inspiration with the same scanner type. However, to assure comparability among different studies, the size distribution of the lesions needs to be considered, especially the frequency of small lesions (28). Chandarana

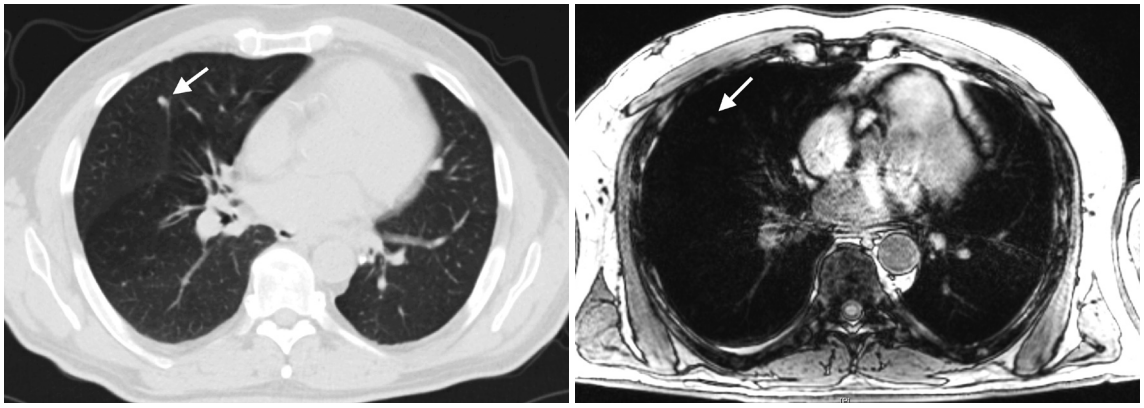

A B

Fig. 5. 62-year-old male patient with thyroid cancer.
A. CT in inspiration. **B.** VIBE in inspiration. In both modalities, lesion in right lung was identified (arrow). In MRI, lesion was assigned to middle lobe, in CT to upper lobe. This was attributed to non-visibility of pulmonary fissure in MRI, which may generally hamper lobe assignment in MRI especially in patients with accessory fissures or fissure distortions. In follow-up imaging, lesion grew in size and was rated as metastasis in standard of reference. VIBE = volume interpolated breath-hold examination

Table 4. Comparison of Figures of Merit (FOM) Obtained by Different Imaging Techniques

	FOM (CI)	Pairwise Comparisons			
		CTex	VIBEin	VIBEex	Dixon
CTex	0.82 (0.70–0.93)	-	0.0008	0.0003	< 0.0001
VIBEin	0.55 (0.40–0.71)	0.0008	-	0.7588	0.0008
VIBEex	0.53 (0.39–0.68)	0.0003	0.7588	-	0.0021
Dixon	0.29 (0.13–0.46)	< 0.0001	0.0008	0.0021	-

FOM are given with 95% confidence intervals (CI) in brackets. *P* values for pairwise comparisons between different imaging techniques are given. CTex = CT acquired in expiration, VIBEex = volume interpolated breath-hold examination acquired in expiration, VIBEin = volume interpolated breath-hold examination acquired in inspiration

Korean Journal of Radiology
KJR

et al. (26) included 25 lesions < 5 mm (36% of all lesions evaluated); while Rauscher et al. (27) used ranges below and above 1 cm for evaluation. Moreover, there may be differences between the acquired and reconstructed voxel size reported in the literature, which is important when evaluating small pulmonary nodules. Besides, the size measurement of lung nodules can be significantly affected by respiration-related changes in lung volume (29).

Early in the evolution of MR/PET, the Dixon sequence for AC was hypothesized to contribute to a morphological identification of FDG-avid lesions (15, 30). However, Rauscher et al. (27) reported low detection rates for the Dixon sequence (32%). In the present study, the lesion-based detection rate for lung nodules was even lower (22%) and 3 patients with malignant pulmonary lesions were missed in the Dixon sequence. In 1 of these 3 patients, the PET information allowed for correct identification of the malignant lesion. The Dixon sequence required for AC is recorded with a relatively low matrix size (determined by the vendor) and cannot be recommended as a sufficient diagnostic option in staging of cancer patients. In contrast, all patients with malignant lesions were identified using dedicated VIBE sequences, irrespective of the breath-hold position.

The reference standard is a critical issue when interpreting comparison studies for pulmonary lesion detection. Stolzmann et al. (31) analysed 66 lesions in 40 patients and found almost comparable detection rates in MRI and CT with the low-dose CT of PET/CT acquired under shallow breathing as reference. In our study, a high-resolution CT in inspiration was the reference standard, which might explain the inferiority of MRI compared to CT.

Another influencing factor for lung nodule evaluation can be the sequence weighting used for lung imaging. Schaarschmidt et al. (32) compared different sequences for T staging in 28 non-small-cell lung cancer patients and found high accuracy for T2-BLADE (proprietary name for periodically rotated overlapping parallel lines with enhanced reconstruction) and T2-half-Fourier acquisition single-shot turbo spin-echo (HASTE) sequences possibly attributable to superior tumor delineation; however, they did not perform a size-based analysis, which limits direct

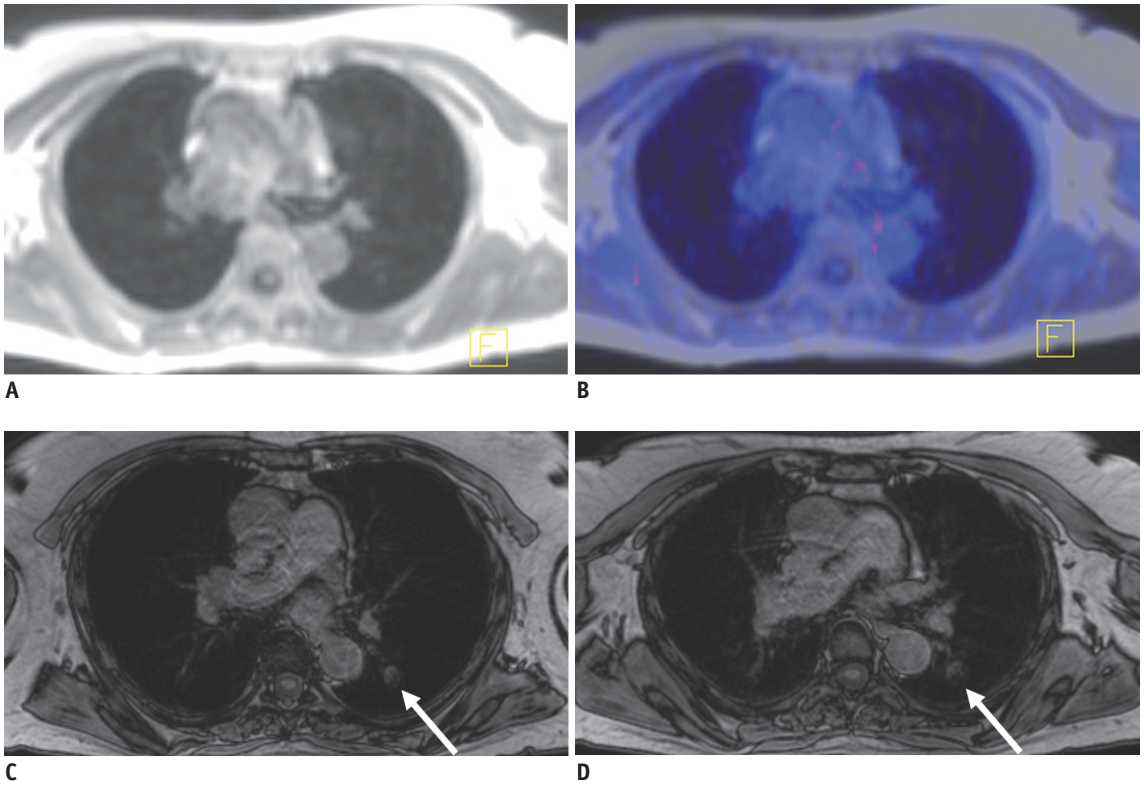

Fig. 6. 76-year-old female patient with thyroid cancer.
A. Dixon sequence in expiration. **B.** Fused PET/Dixon. **C.** VIBEin. **D.** VIBEex. In VIBE images, pulmonary lesion was found both in inspiratory and expiratory scan (arrow). In Dixon sequence, lesion was not adequately visible and scan was rated as negative. Also in fused PET/Dixon images, lesion was not identifiable. Lesion was classified as malignant based on standard of reference due to growth in size in follow-up imaging. PET = positron emission tomography, VIBE = volume interpolated breath-hold examination, VIBEex = volume interpolated breath-hold examination acquired in expiration, VIBEin = volume interpolated breath-hold examination acquired in inspiration

comparison. Although T2-weighted sequences are reportedly beneficial for pulmonary lesion characterization (33), their relatively long acquisition time and the concomitant need for respiratory and/or cardiac gating may interfere with patient compliance and smooth workflow in routine MR/PET schedules. Therefore, dedicated 3D VIBE sequences have been preferred for lung evaluation in oncologic MR/PET, since they can be performed within one breath-hold and have been reported to provide excellent results in lung staging compared with PET/CT (34).

Interestingly, in 2 cases, false diagnosis of lobe involvement was made in MRI because lung fissures essential for correct lobe attribution were not clearly visible. This is important in lung staging when lobe involvement can make a difference in T staging (separate tumor nodule in the same lobe versus separate tumour nodule in different ipsilateral lobe). However, in our study, the false lobe attribution that occurred in 2 metastatic thyroid cancer patients did not alter the overall staging and treatment strategy.

In our study, follow-up examination or biopsy was available for 47 lesions in 17 patients. 33 of those 47 lesions were malignant. Considering only these malignant lesions, the detection rates increased for all modalities. It is important to note, that the median lesion size of these malignant lesions was smaller compared to all lesions (median lesion size: 6 mm vs. 8 mm). This is in accordance with the literature where many small pulmonary nodules are reported to be benign even in oncologic patients (35).

Our study has limitations. First, no intravenous contrast media was used for MR imaging. Lee et al. (36) reported that the application of contrast media did not provide additional value in the detection rate of pulmonary nodules. However, the use of dynamic contrast-enhanced imaging might be helpful in the differentiation between benign and malignant nodules. Acquisition of dynamic series, however, accompanies an increase in acquisition time. Second, in this study set-up, we merely included fast T1-weighted sequences and did not evaluate T2-weighted sequences or gradient-echo sequences with radial stack-of-stars trajectory because the latter have acquisition times of several minutes. Our study was focused on fast sequences that can smoothly be integrated in an oncologic whole-body MR/PET protocol. Third, the reconstruction parameters of CTin and CTex differed because CTex was part of the whole-body acquisition while CTin was a dedicated lung scan. These CT reconstructions are part of the routine clinical PET/CT protocol, which was not explicitly changed for this retrospective comparison study. However, the analysis of the CT in expiration was not the primary scope of the study designed to investigate the diagnostic performance of fast dedicated MR sequences used for pulmonary lesion evaluation in oncologic MR/PET patients. Fourth, there is a selection bias due to the retrospective evaluation of the imaging data and the patient number was rather small limiting the representativeness for a general oncology patient collective. Finally, histological correlation was not available for each single lesion. This is not realizable in patients with numerous small lung nodules for obvious reasons. However, we included a separate analysis of diagnostic performance considering only malignant pulmonary lesions, which were confirmed by follow-up or biopsy.

In conclusion, the value of fast T1-weighted sequences used for lung nodule assessment in MR/PET imaging of cancer patients depends on the evaluation strategy: in a lesion-based comparison, MRI clearly remains inferior to CT irrespective of the breath-hold position with very low detection rates for small (< 4 mm) lung nodules. However, the diagnostic performance of fast VIBE sequences improves when moving to lobe- or patient-based analyses, which may represent a more treatment-orientated evaluation strategy. Fast T1-weighted VIBE sequences as routinely available in MR/PET protocols allow for reliable identification of patients with malignant pulmonary lesions. The Dixon sequence routinely included for AC cannot be considered adequate for lung nodule evaluation in cancer patients irrespective of the evaluation strategy (lesion-/lobe-/size-based) due to the poor detection rate and the low confidence in lesion delineation. In contrast to CT, the breath-hold position does not substantially alter the detection rate for lung nodules in fast T1-weighted VIBE sequences in MR/PET but plays an important role for the diagnostic confidence in lesion delineation.

Acknowledgments

The authors thank PD Dr. Brigitte Gueckel for her constant support and Gerd Zeger and Carsten Groeper for their continuous efforts regarding organisation and image acquisition in the PET/MR unit.

The Department of Radiology of the University Hospital in Tuebingen has a collaboration contract with Siemens Healthcare concerning technical development of PET/MR.

Korean Journal of Radiology
KJR

REFERENCES

1. Yoo HJ, Lee JS, Lee JM. Integrated whole body MR/PET: where are we? *Korean J Radiol* 2015;16:32-49
2. Catalano OA, Rosen BR, Sahani DV, Hahn PF, Guimaraes AR, Vangel MG, et al. Clinical impact of PET/MR imaging in patients with cancer undergoing same-day PET/CT: initial experience in 134 patients--a hypothesis-generating exploratory study. *Radiology* 2013;269:857-869
3. Boss A, Weiger M, Wiesinger F. Future image acquisition trends for PET/MRI. *Semin Nucl Med* 2015;45:201-211
4. Gatidis S, Schmidt H, Gückel B, Bezrukov I, Seitz G, Ebinger M, et al. Comprehensive oncologic imaging in infants and preschool children with substantially reduced radiation exposure using combined simultaneous ^{18}F-fluorodeoxyglucose positron emission tomography/magnetic resonance imaging: a direct comparison to ^{18}F-fluorodeoxyglucose positron emission tomography/computed tomography. *Invest Radiol* 2016;51:7-14
5. Grueneisen J, Schaarschmidt BM, Heubner M, Suntharalingam S, Milk I, Kinner S, et al. Implementation of FAST-PET/MRI for whole-body staging of female patients with recurrent pelvic malignancies: a comparison to PET/CT. *Eur J Radiol* 2015;84:2097-2102
6. Manber R, Thielemans K, Hutton BF, Barnes A, Ourselin S, Arridge S, et al. Practical PET respiratory motion correction in clinical PET/MR. *J Nucl Med* 2015;56:890-896
7. Würslin C, Schmidt H, Martirosian P, Brendle C, Boss A, Schwenzer NF, et al. Respiratory motion correction in oncologic PET using T1-weighted MR imaging on a simultaneous whole-body PET/MR system. *J Nucl Med* 2013;54:464-471
8. Biederer J, Beer M, Hirsch W, Wild J, Fabel M, Puderbach M, et al. MRI of the lung (2/3). Why … when … how? *Insights Imaging* 2012;3:355-371
9. Wild JM, Marshall H, Bock M, Schad LR, Jakob PM, Puderbach M, et al. MRI of the lung (1/3): methods. *Insights Imaging* 2012;3:345-353
10. Chandarana H, Block TK, Rosenkrantz AB, Lim RP, Kim D, Mossa DJ, et al. Free-breathing radial 3D fat-suppressed T1-weighted gradient echo sequence: a viable alternative for contrast-enhanced liver imaging in patients unable to suspend respiration. *Invest Radiol* 2011;46:648-653
11. Raad RA, Friedman KP, Heacock L, Ponzo F, Melsaether A, Chandarana H. Outcome of small lung nodules missed on hybrid PET/MRI in patients with primary malignancy. *J Magn Reson Imaging* 2016;43:504-511
12. Bader TR, Semelka RC, Pedro MS, Armao DM, Brown MA, Molina PL. Magnetic resonance imaging of pulmonary parenchymal disease using a modified breath-hold 3D gradient-echo technique: initial observations. *J Magn Reson Imaging* 2002;15:31-38
13. Biederer J, Schoene A, Freitag S, Reuter M, Heller M. Simulated pulmonary nodules implanted in a dedicated porcine chest phantom: sensitivity of MR imaging for detection. *Radiology* 2003;227:475-483
14. Fink C, Puderbach M, Biederer J, Fabel M, Dietrich O, Kauczor HU, et al. Lung MRI at 1.5 and 3 Tesla: observer preference study and lesion contrast using five different pulse sequences. *Invest Radiol* 2007;42:377-383
15. Eiber M, Martinez-Möller A, Souvatzoglou M, Holzapfel K, Pickhard A, Löffelbein D, et al. Value of a Dixon-based MR/PET attenuation correction sequence for the localization and evaluation of PET-positive lesions. *Eur J Nucl Med Mol Imaging* 2011;38:1691-1701
16. Gilman MD, Fischman AJ, Krishnasetty V, Halpern EF, Aquino SL. Optimal CT breathing protocol for combined thoracic PET/CT. *AJR Am J Roentgenol* 2006;187:1357-1360
17. Juergens KU, Weckesser M, Stegger L, Franzius C, Beetz M, Schober O, et al. Tumor staging using whole-body high-resolution 16-channel PET-CT: does additional low-dose chest CT in inspiration improve the detection of solitary pulmonary nodules? *Eur Radiol* 2006;16:1131-1137
18. de Juan R, Seifert B, Berthold T, von Schulthess GK, Goerres GW. Clinical evaluation of a breathing protocol for PET/CT. *Eur Radiol* 2004;14:1118-1123
19. Goerres GW, Kamel E, Heidelberg TN, Schwitter MR, Burger C, von Schulthess GK. PET-CT image co-registration in the thorax: influence of respiration. *Eur J Nucl Med Mol Imaging* 2002;29:351-360
20. MacMahon H, Austin JH, Gamsu G, Herold CJ, Jett JR, Naidich DP, et al. Guidelines for management of small pulmonary nodules detected on CT scans: a statement from the Fleischner Society. *Radiology* 2005;237:395-400
21. Chakraborty DP. Analysis of location specific observer performance data: validated extensions of the jackknife free-response (JAFROC) method. *Acad Radiol* 2006;13:1187-1193
22. Chakraborty DP, Berbaum KS. Observer studies involving detection and localization: modeling, analysis, and validation. *Med Phys* 2004;31:2313-2330
23. Vogel MN, Brechtel K, Klein MD, Aschoff P, Horger M, Eschmann S, et al. [Evaluation of different breathing and contrast-protocols concerning quality and alignment in 18F-FDG PET/CT]. *Rofo* 2007;179:72-79
24. Allen-Auerbach M, Yeom K, Park J, Phelps M, Czernin J. Standard PET/CT of the chest during shallow breathing is inadequate for comprehensive staging of lung cancer. *J Nucl Med* 2006;47:298-301
25. Aquino SL, Kuester LB, Muse VV, Halpern EF, Fischman AJ. Accuracy of transmission CT and FDG-PET in the detection of small pulmonary nodules with integrated PET/CT. *Eur J Nucl Med Mol Imaging* 2006;33:692-696
26. Chandarana H, Heacock L, Rakheja R, DeMello LR, Bonavita J, Block TK, et al. Pulmonary nodules in patients with primary malignancy: comparison of hybrid PET/MR and PET/CT imaging. *Radiology* 2013;268:874-881
27. Rauscher I, Eiber M, Fürst S, Souvatzoglou M, Nekolla SG, Ziegler SI, et al. PET/MR imaging in the detection and characterization of pulmonary lesions: technical and diagnostic evaluation in comparison to PET/CT. *J Nucl Med*

2014;55:724-729
28. Heye T, Ley S, Heussel CP, Dienemann H, Kauczor HU, Hosch W, et al. Detection and size of pulmonary lesions: how accurate is MRI? A prospective comparison of CT and MRI. *Acta Radiol* 2012;53:153-160
29. Goo JM, Kim KG, Gierada DS, Castro M, Bae KT. Volumetric measurements of lung nodules with multi-detector row CT: effect of changes in lung volume. *Korean J Radiol* 2006;7:243-248
30. Drzezga A, Souvatzoglou M, Eiber M, Beer AJ, Fürst S, Martinez-Möller A, et al. First clinical experience with integrated whole-body PET/MR: comparison to PET/CT in patients with oncologic diagnoses. *J Nucl Med* 2012;53:845-855
31. Stolzmann P, Veit-Haibach P, Chuck N, Rossi C, Frauenfelder T, Alkadhi H, et al. Detection rate, location, and size of pulmonary nodules in trimodality PET/CT-MR: comparison of low-dose CT and Dixon-based MR imaging. *Invest Radiol* 2013;48:241-246
32. Schaarschmidt B, Buchbender C, Gomez B, Rubbert C, Hild F, Köhler J, et al. Thoracic staging of non-small-cell lung cancer using integrated (18)F-FDG PET/MR imaging: diagnostic value of different MR sequences. *Eur J Nucl Med Mol Imaging* 2015;42:1257-1267
33. Sommer G, Tremper J, Koenigkam-Santos M, Delorme S, Becker N, Biederer J, et al. Lung nodule detection in a high-risk population: comparison of magnetic resonance imaging and low-dose computed tomography. *Eur J Radiol* 2014;83:600-605
34. Fraioli F, Screaton NJ, Janes SM, Win T, Menezes L, Kayani I, et al. Non-small-cell lung cancer resectability: diagnostic value of PET/MR. *Eur J Nucl Med Mol Imaging* 2015;42:49-55
35. Munden RF, Erasmus JJ, Wahba H, Fineberg NS. Follow-up of small (4 mm or less) incidentally detected nodules by computed tomography in oncology patients: a retrospective review. *J Thorac Oncol* 2010;5:1958-1962
36. Lee KH, Park CM, Lee SM, Lee JM, Cho JY, Paeng JC, et al. Pulmonary nodule detection in patients with a primary malignancy using hybrid PET/MRI: is there value in adding contrast-enhanced MR imaging? *PLoS One* 2015;10:e0129660